

Electronic Supplemental Information

Meso-N-methylation of a porphyrinoid complex: Activating the H-atom transfer capability of an inert Re^V(O) corrolazine

*Evan E. Joslin, Jan Paulo T. Zaragoza, Maxime A. Siegler, and David P. Goldberg**

Department of Chemistry, The Johns Hopkins University, 3400 N. Charles Street, Baltimore,
MD 21218, USA

*Email: dgp@jhu.edu

General Procedures. All reactions were performed using dry solvents and standard Schlenk techniques unless otherwise noted. Dichloromethane and toluene were purified via a Pure-Solv solvent purification system from Innovative Technologies. CD₂Cl₂ was obtained from Cambridge Isotopes, Inc. The synthesis of Re^V(O)(TBP₈Cz) (TBP₈Cz = octakis(*p*-*tert*-butylphenyl)corrolazinato),¹ [H(OEt₂)₂]⁺[B(C₆F₅)₄]⁻ (HBArF),² 2,2,6,6-tetramethylpiperidine hydroxylamine (TEMPOH)³ and its deuterated analogue TEMPOD, followed published literature procedures. All other reagents were purchased from commercial sources and used without further purification.

Instrumentation. ¹H NMR spectra were recorded on a Bruker Avance 400 MHz or a Bruker Avance 600 MHz spectrometer. All ¹H spectra were referenced against residual solvent proton signals. ¹⁹F NMR spectra were recorded on a Bruker 300 MHz (operating frequency 282 MHz) spectrometer and referenced against an external standard of C₆F₆ (δ = -164.9 ppm). Electron paramagnetic resonance (EPR) spectra were recorded with a Bruker EMX spectrometer equipped with a Bruker ER 041 X G microwave bridge. Elemental analyses were performed at Atlantic Microlab, Inc. in Norcross, GA. Electrochemical experiments were performed under an argon atmosphere using a BAS 100B electrochemical analyzer. Cyclic voltammograms were recorded in degassed CH₂Cl₂ using a standard three-electrode system consisting of a glassy carbon working electrode, a Ag/AgNO₃ non-aqueous reference electrode (0.01 M AgNO₃ with 0.1 M TBAPF₆ in CH₃CN), and a platinum wire counter electrode and tetrabutylammonium hexafluorophosphate (TBAPF₆, 0.1 M) as supporting electrolyte. All potentials are reported versus Fc⁺/Fc. UV-vis measurements were performed on a Hewlett-Packard 8453 diode-array spectrophotometer with a 3.5 mL air-free quartz cuvette (path length = 1 cm) fitted with a glass stopper or rubber septum. A 400 nm longpass filter was employed to prevent photo-

decomposition by placing the filter directly between the sample quartz cuvette and the spectrophotometer light source. LDI-MS was collected on a Bruker Autoflex III/TOF/TOF instrument equipped with a nitrogen laser at 335 nm using an MTP 384 ground steel target plate. ATR-IR spectra were collected from a ThermoNicolet Nexus 670 FTIR Spectrometer equipped with a KRS-5 ATR. IR samples were dissolved in a minimal amount of CH₂Cl₂ and spotted on the ATR and allowed to dry prior to collecting data.

Computational Methods. Computational studies on the rhenium complexes were performed using the *Orca* program package.⁴ Geometry optimizations and frequency calculations were performed using the hybrid density functional theory PBE0^{5,6} with the LANL2TZ⁷ basis set on Re and the 6-31G**^{8,9} basis set on the remaining atoms, as suggested by Deakyne, and co-workers¹⁰ for monooxorhenium(V) complexes. The initial geometry of the rhenium-oxo corrolazine ¹[Re^V(O)(CzH₆P₂)], (CzH₆P₂ = diphenylcorrolazinato) was obtained from the Re^V(O)(TBP₈Cz) X-ray crystal structure with six of the *p-tert*-butylphenyl groups replaced with hydrogens, and the two closest to one *meso*-N replaced with phenyls to account for the steric strain upon methylation. Subsequent calculations were achieved by manually adding a proton or a methyl group on the *meso*-N position of the corrolazine ligand, and adding or removing an electron, then allowing the structures to optimize without constraints. Optimized geometries were used for frequency calculations at the same level of theory to ensure the local minimum nature of the geometry (without any imaginary frequencies).

[Re^V(O)(*N*-MeTBP₈Cz)]⁺[OTf]⁻ (1). An amount of Re^V(O)(TBP₈Cz) (0.014 g, 0.0091 mmol) was dissolved in 5 mL of toluene. MeOTf (51 μL, 0.45 mmol) was added by syringe and the reaction was refluxed for 12 h during which time the solution turned from bright green to red-brown. Additional MeOTf (51 μL, 0.45 mmol) was added to the reaction mixture and the

reaction mixture was allowed to reflux for another 12 h. The reaction was cooled to 23 °C and the solvent was removed via rotary vacuum. The residual solid was dissolved in a minimal amount of CH₂Cl₂ and loaded onto a silica gel preparatory plate. The plate was developed with CH₂Cl₂/EtOAc (8:2 v/v). The brown band (R_f = 0.08) was scraped off the plate and the silica was placed in a CH₂Cl₂/EtOAc (8:2 v/v) solution to solubilize the product. The silica was then removed by filtration and the solution was dried under vacuum to yield a brown-red solid (0.0059 g, 38 % yield). ¹H NMR (400 MHz, CD₂Cl₂) δ 8.34 (dd, ³J_{HH} = 8, 6 Hz, 4H, Ar-H), 8.14 (d, ³J_{HH} = 8 Hz, 3H, Ar-H), 7.99 (d, ³J_{HH} = 8 Hz, 2H, Ar-H), 7.75-7.46 (m, 16H, Ar-H), 7.28 (bs, 3H, Ar-H), 7.23 (d, ³J_{HH} = 8 Hz, 2H, Ar-H), 7.07 (d, ³J_{HH} = 8 Hz, 2H, Ar-H), 5.01 (s, 3H, meso-CH₃), 1.52 (s, 9H, Ph-C(CH₃)₃), 1.50 (s, 9H, Ph-C(CH₃)₃), 1.47 (2s overlapping, 18H, Ph-C(CH₃)₃), 1.44 (s, 9H, Ph-C(CH₃)₃), 1.39 (s, 9H, Ph-C(CH₃)₃), 1.36 (s, 9H, Ph-C(CH₃)₃), 1.26 (s, 9H, Ph-C(CH₃)₃). ¹⁹F NMR (282 MHz, CD₂Cl₂) δ -81.22. UV-Vis (CH₂Cl₂) λ_{max} [nm] (ε × 10⁻⁴) 464 (4.9), 732 (2.5). FT-IR (cm⁻¹, ATR) 1463, 1363, 1270, 1252, 1161, 1108, 1030, 1001, 984, 837. MS (MALDI) *m/z* = 1572.53 (M⁺). Anal. Calcd. for C₉₈H₁₀₇F₃N₇O₄ReS•CH₂Cl₂•EtOAc: C, 65.27; H, 6.22; N, 5.17. Found: C, 65.01; H, 6.58; N, 4.84.

[Re^V(O)(N-MeTBP₈Cz-H)]²⁺[BArF]₂. [Re^V(O)(N-MeTBP₈Cz)]⁺[OTf]⁻ (**1**) (0.0027 g, 0.0016 mmol) was dissolved in *c.a.* 1 mL of CH₂Cl₂, and HBarF (0.0027 g, 0.0033 mmol) was added, causing a color change from dark brown to bright pink. The solution was placed in an NMR tube and layered with *n*-heptane, and afforded X-ray quality crystals after approximately 1 month.

Single Crystal X-ray Crystallography. All reflection intensities were measured at 110(2) K for [Re^V(O)(N-MeTBP₈Cz)(H)]²⁺[BArF]₂ (**2**) using a SuperNova diffractometer (equipped with Atlas detector) with Cu K α radiation (λ = 1.54178 Å) under the program CrysAlisPro (Version

1.171.36.32, Agilent Technologies, 2013). The same program was used to refine the cell dimensions and for data reduction. The structure was solved with the program SHELXS-2014/7 and was refined on F^2 with SHELXL-2014/7.¹¹ Analytical numeric absorption correction using a multifaceted crystal model was applied using CrysAlisPro. The temperature of the data collection was controlled using the system Cryojet (manufactured by Oxford Instruments). The H atoms were placed at calculated positions using the instructions AFIX 23, AFIX 43, AFIX 137 with isotropic displacement parameters having values 1.2 or 1.5 U_{eq} of the attached C atoms. Crystallographic data for $[\text{Re}^{\text{V}}(\text{O})(N\text{-MeTBP}_8\text{Cz})(\text{H})]^{2+}[\text{BARF}]_2^-$ has been deposited with the Cambridge Crystallographic Data Center (CCDC) with the deposition number of 1510757.

Six of the eight *para*-tert-butylphenyl groups and one of the two BARF counterions are found to be disordered over two orientations. All occupancy factors are provided in the .cif file. The crystal lattice also includes disordered heptane lattice solvent molecules. Two molecules (one is found at a site of inversion symmetry and its occupancy factor was constrained to be 0.5) have been added into the structure model, but the remaining contribution of the third heptane solvent molecule was removed in the final refinement using the SQUEEZE procedure in Platon.¹²

Additional Note: checkCIF shows one Alert Level B “Large U3/U1 Ratio for Average U(i,j) Tensor”. Although it is a bit unusual, it might be inherently due to the long range order in the crystal, as there seems to be some significant amount of disorder in the crystal lattice. This alert does not affect the validity of the model.

General Procedure for EPR Spectroscopy. To an amount of $[\text{Re}^{\text{V}}(\text{O})(N\text{-MeTBP}_8\text{Cz})]^{+}[\text{OTf}]^{-}$ (**1**) (0.2 - 0.89 mM) dissolved in CH_2Cl_2 was added phenylhydrazine (0.56 - 1.6 M) in CH_2Cl_2 . A subtle color change from brown to red-brown was observed and the completion of the reaction was checked by UV-vis spectroscopy. The solution was loaded into

an EPR tube, and an EPR spectrum was obtained. EPR parameters: T = 294 K, freq. = 9.77 GHz, power = 2.012 mW, mod. amp. = 1 G, mod. freq. = 100 kHz, receiver gain = 5.02×10^3 , NS = 2.

UV-vis kinetics for the reaction of $[\text{Re}^{\text{V}}(\text{O})(\text{N-MeTBP}_8\text{Cz})]^+[\text{OTf}]^-$ (1**) with TEMPOH(D).** $[\text{Re}^{\text{V}}(\text{O})(\text{N-MeTBP}_8\text{Cz})]^+[\text{OTf}]^-$ (**1**) (13 μM , CH_2Cl_2) was reacted with TEMPOH(D) (0.03 – 0.18 M). The reaction was monitored by UV-vis spectroscopy and showed the decay of $[\text{Re}^{\text{V}}(\text{O})(\text{N-MeTBP}_8\text{Cz})]^+[\text{OTf}]^-$ (**1**) ($\lambda_{\text{max}} = 467, 732 \text{ nm}$) and production of $[\text{Re}^{\text{V}}(\text{O})(\text{N-MeTBP}_8\text{Cz})]^+$ (**3**) ($\lambda_{\text{max}} = 440, 489, 920 \text{ nm}$). The pseudo first order rate constants, k_{obs} , were obtained by nonlinear least-squares fitting of the growth of $[\text{Re}^{\text{V}}(\text{O})(\text{N-MeTBP}_8\text{Cz})]^+$ (**3**) and decay of $[\text{Re}^{\text{V}}(\text{O})(\text{N-MeTBP}_8\text{Cz})]^+[\text{OTf}]^-$ (**1**) plotted as absorbance (Abs) versus time (t). The data were fit to the equation $\text{Abs}_t = \text{Abs}_f + (\text{Abs}_0 - \text{Abs}_f)\exp(-k_{\text{obs}}t)$, where Abs_0 and Abs_f are initial and final absorbance, respectively. Pseudo-first order k_{obs} values were obtained and exhibited a linear correlation with substrate concentrations. Second-order rate constants (k_2) were obtained from the slope of the best-fit line from a plot of k_{obs} versus substrate concentration.

Table S1. Comparison of Selected Bond Distances (Å) and Angles (deg) for $[\text{Re}^{\text{V}}(\text{O})(\text{N-MeTBP}_8\text{Cz})(\text{H})]^{2+}[\text{BArF}]_2^-$ (**2**) and $\text{Re}^{\text{V}}(\text{O})(\text{TBP}_8\text{Cz})$.¹

	$[[\text{Re}^{\text{V}}(\text{O})(\text{N-MeTBP}_8\text{Cz})(\text{H})]^{2+}[\text{BArF}]_2^-$ (2)	$\text{Re}^{\text{V}}(\text{O})(\text{TBP}_8\text{Cz})$
Re–O	1.6643(17)	1.682(5)
Re–N _{ave}	1.991	1.976
Re–(N _{pyrrole}) _{plane}	0.744	0.739
Re–(23-atom) _{core}	0.959	1.00
N–CH3	1.497(4)	--
C1–N7	1.362(3)	1.294(10)
C16–N7	1.376(4)	1.299(10)
C1–N7–CH3	117.9(2)	--
C16–N7–CH3	117.7(2)	--
C1–N7–C16	124.3(2)	--
C α –C α (C4–C5)	1.402(3)	1.522(9)
N1–Re1–N2	75.06(8)	76.8(4)
N2–Re1–N4	83.43(8)	84.6(3)
N4–Re1–N6	86.59(9)	84.7(3)
N6–Re1–N1	82.73(8)	81.8(4)

Table S2. Calculated vibrational modes for $\text{Re}^{\text{V}}(\text{O})$ complexes. Relevant $\nu(\text{Re-O})$ modes are highlighted in red.

	$^1[\text{Re}^{\text{V}}(\text{O})(\text{CzH}_6\text{P}_2)]$	$^1[\text{Re}^{\text{V}}(\text{O})(\text{CzH}_6\text{P}_2)(\text{CH}_3)]^+$
Mode	Freq. (cm ⁻¹)	Freq. (cm ⁻¹)
7	36.71	
8	40.66	37.9
9	49.8	43.68
10	58.17	47.43
11	85.95	71.59
12	90.36	87.18
13	99.11	92.16
14	120.88	105.52
15	139.65	130.35
16	144.6	137.55
17	185.22	144.23
18	190.01	158.72
19	201.39	178.6
20	224.19	188.96
21	230.69	214.2
22	238.75	224.81
23	249.74	235.22
24	253.25	239.79

25	274.69	242.99
26	283.22	251.89
27	297.9	272.32
28	306.5	281.82
29	324.13	287.44
30	330.64	310.42
31	358.54	322.9
32	391.98	333.66
33	398.1	379.04
34	412.19	393.05
35	414.15	409.45
36	417.9	413.55
37	454.75	414.65
38	462.59	424.86
39	476.09	430.68
40	483.57	437.24
41	494.58	452.03
42	514.21	466.7
43	532.79	472.54
44	549.84	482.87
45	588.95	510.37
46	605.45	534.05
47	612.72	547.26
48	630.57	559.04
49	632.14	584.32
50	653.41	601.44
51	677.7	627.14
52	685.98	629.42
53	696.12	650.95
54	699.12	658.54
55	707.82	679.64
56	710.56	693.42
57	716.98	694.16
58	733.55	711.19
59	741.46	718.99
60	743.18	721.1
61	748.63	722.58
62	762.37	734.18
63	768.95	741.89
64	790.15	744.39
65	792.85	748.5

66	798.06	753.73
67	808.47	778.57
68	810.48	787.93
69	828.32	795.82
70	842.61	804.24
71	856.07	818.3
72	858.8	826.59
73	864.76	841.44
74	872.85	849.94
75	882.81	866.92
76	917.26	870.91
77	921.14	884.73
78	939.66	892.44
79	943.92	918.21
80	944.75	947.99
81	982.7	949.23
82	988.37	949.6
83	1004.71	962.62
84	1010.16	991.64
85	1018.48	991.85
86	1018.64	993.65
87	1030.42	1016.93
88	1047.9	1019.5
89	1053.63 (Re-O)	1022.72
90	1055.22	1023.55
91	1058.32	1023.79
92	1062.27	1044.85
93	1064.73	1056.97
94	1076.08	1063.43 (Re-O)
95	1083.05	1064.2
96	1084.75	1072.2
97	1094	1076.01
98	1116.17	1077.22
99	1118.35	1087.1
100	1122.07	1090.38
101	1169.02	1116.07
102	1187.67	1116.31
103	1188.27	1120.49
104	1197.08	1140.32
105	1212.85	1152.99
106	1214.73	1157.27

107	1242.5	1171.95
108	1254.99	1192.7
109	1272.19	1193.98
110	1284.94	1209.4
111	1299.58	1210.22
112	1311.8	1220.52
113	1334.14	1249.13
114	1340.47	1257.98
115	1344.16	1280.51
116	1361.1	1285.01
117	1376.52	1308.56
118	1386.34	1329.23
119	1388.42	1335.56
120	1393.12	1339.67
121	1402.48	1341.69
122	1439.98	1362.95
123	1443.02	1368.04
124	1481.26	1380.4
125	1488.6	1381.63
126	1491.28	1389.13
127	1500.63	1398.76
128	1515.37	1426.8
129	1523.9	1440.16
130	1542.33	1449.9
131	1553.69	1473.19
132	1561.86	1489.78
133	1575.93	1492.37
134	1580.09	1497.69
135	1593.04	1501.71
136	1604.74	1507.21
137	1617.19	1517.45
138	1634.39	1520.89
139	1654.43	1529.06
140	1655.85	1547.59
141	1683.31	1564.43
142	1684.36	1571.73
143	3204.77	1583.84
144	3206.94	1594.12
145	3212.88	1609.27
146	3214.57	1619.34
147	3222.02	1644.86

148	3223.83	1653.78
149	3233.5	1654.25
150	3234.85	1679.89
151	3250.65	1680.74
152	3255.3	3125.52
153	3280.5	3205.66
154	3281.29	3208.77
155	3284.58	3216.2
156	3293.57	3217.16
157	3298.42	3225.93
158	3302.38	3226.24
159		3230.23
160		3234.47
161		3235.23
162		3245.13
163		3245.53
164		3253.94
165		3288.26
166		3291.98
167		3292.15
168		3298.92
169		3303.98
170		3308.22
171		
172		
173		

Table S3. Crystallographic Data for **2**.

Crystal data	
Chemical formula	C ₉₇ H ₁₀₈ N ₇ ORe·2(C ₂₄ BF ₂₀)·1.414(C ₇ H ₁₆)
M_r	3073.83
Crystal system, space group	Triclinic, <i>P</i> -1
Temperature (K)	110
a, b, c (Å)	17.92851 (19), 18.50308 (19), 24.9906 (2)
α, β, γ (°)	93.4898 (8), 107.0384 (9), 108.1775 (9)
V (Å ³)	7424.19 (13)
Z	2
Radiation type	Cu $K\alpha$
μ (mm ⁻¹)	2.50
Crystal size (mm)	0.30 × 0.29 × 0.20
Data collection	
Diffractometer	SuperNova, Dual, Cu at zero, Atlas
Absorption correction	Analytical CrysAlis PRO, Agilent Technologies, Version 1.171.36.32 (release 02-08-2013 CrysAlis171 .NET) (compiled Aug 2 2013,16:46:58) Analytical numeric absorption correction using a multifaceted crystal model based on expressions derived by R.C. Clark & J.S. Reid. (R. C. Clark, and J. S. Reid, <i>Acta Cryst.</i> 1995, A51 , 887-897)
T_{\min}, T_{\max}	0.563, 0.715
No. of measured, independent and observed [$I > 2\sigma(I)$] reflections	96114, 29003, 26868
R_{int}	0.026
$(\sin \theta/\lambda)_{\text{max}}$ (Å ⁻¹)	0.617
Refinement	
$R[F^2 > 2\sigma(F^2)], wR(F^2), S$	0.036, 0.098, 1.04
No. of reflections	29003
No. of parameters	2857
No. of restraints	4061
H-atom treatment	H-atom parameters constrained
$\Delta\rho_{\text{max}}, \Delta\rho_{\text{min}}$ (e Å ⁻³)	0.86, -1.21

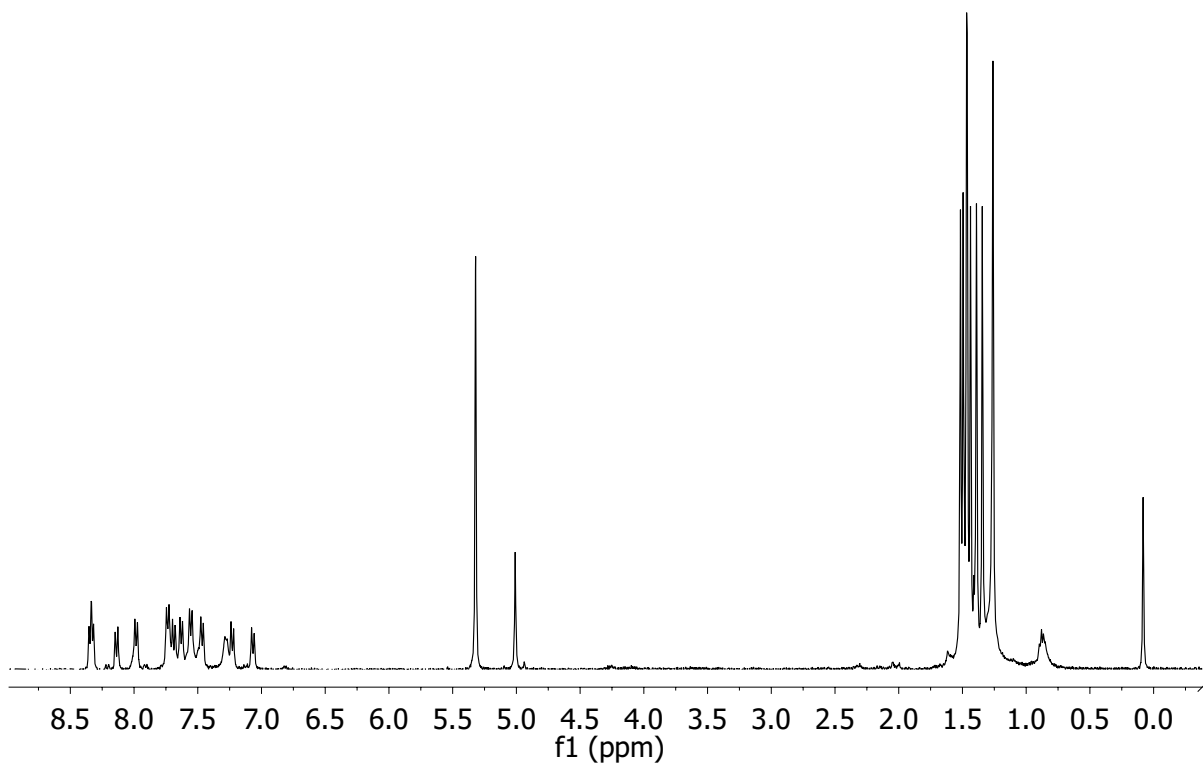


Figure S1. ^1H NMR spectrum of $[\text{Re}^{\text{V}}(\text{O})(N\text{-MeTBP}_8\text{Cz})]^+[\text{OTf}]^-$ (**1**) in CD_2Cl_2 .

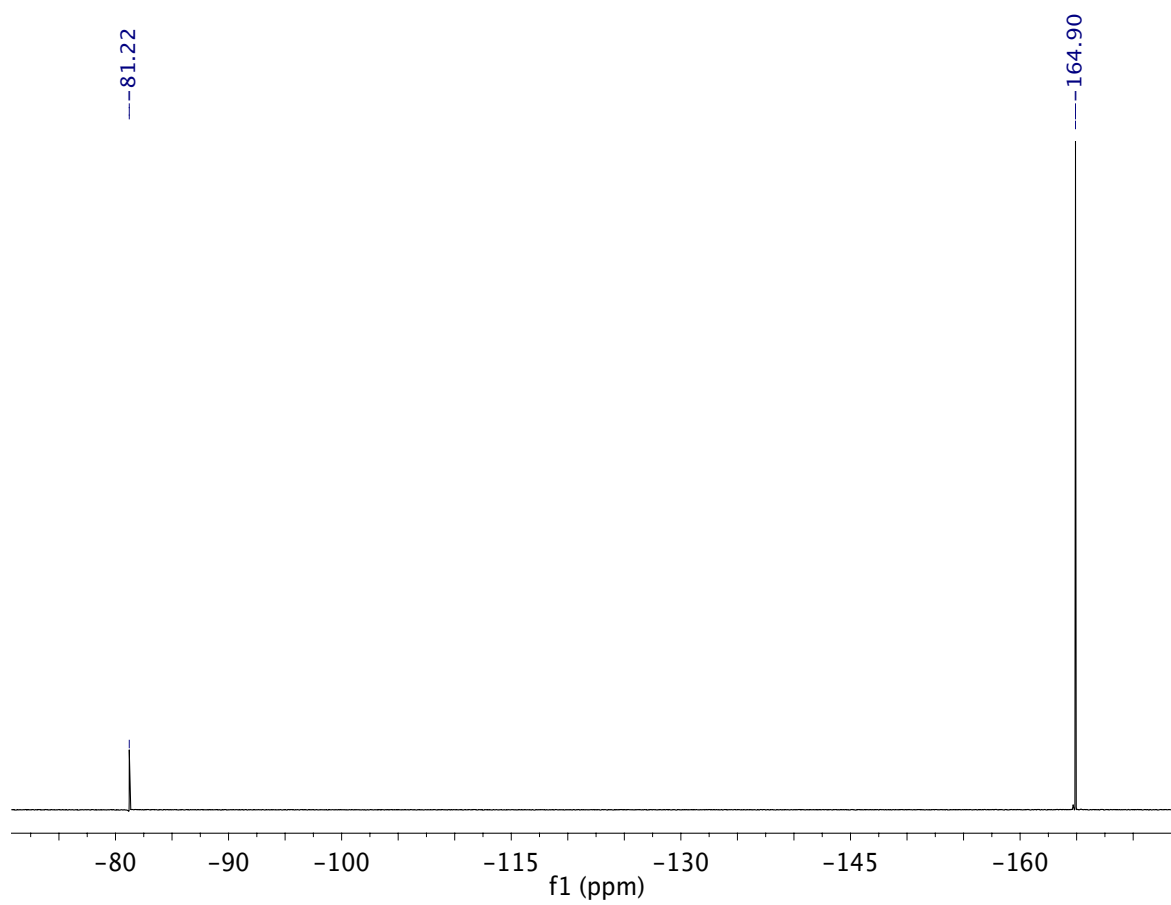


Figure S2. ^{19}F NMR spectrum of $[\text{Re}^{\text{V}}(\text{O})(\text{N-MeTBP}_8\text{Cz})]^+[\text{OTf}]^-$ (**1**) in CD_2Cl_2 . Chemical shifts were calibrated versus the standard C_6F_6 at -164.9 ppm.

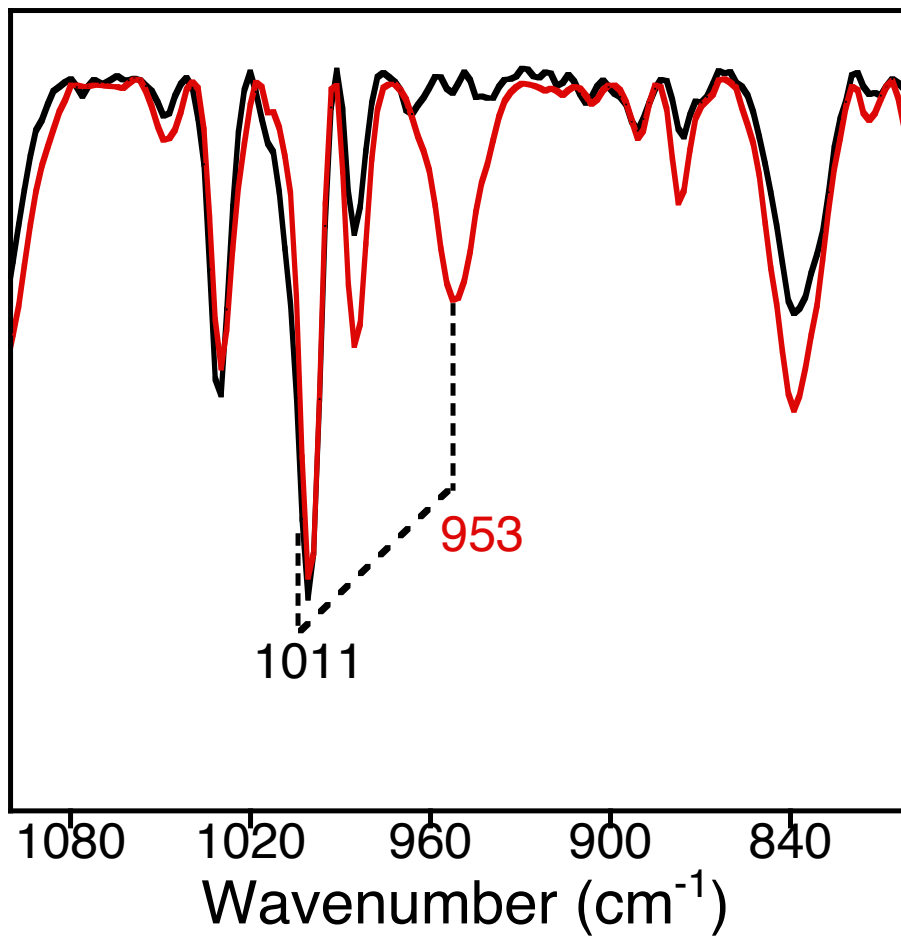


Figure S3. ATR-IR spectra (850 - 1100 cm⁻¹) of [Re^V(¹⁸O)(*N*-MeTBP₈Cz)]⁺[OTf]⁻ (red) and [Re^V(¹⁶O)(*N*-MeTBP₈Cz)]⁺[OTf]⁻ (black).

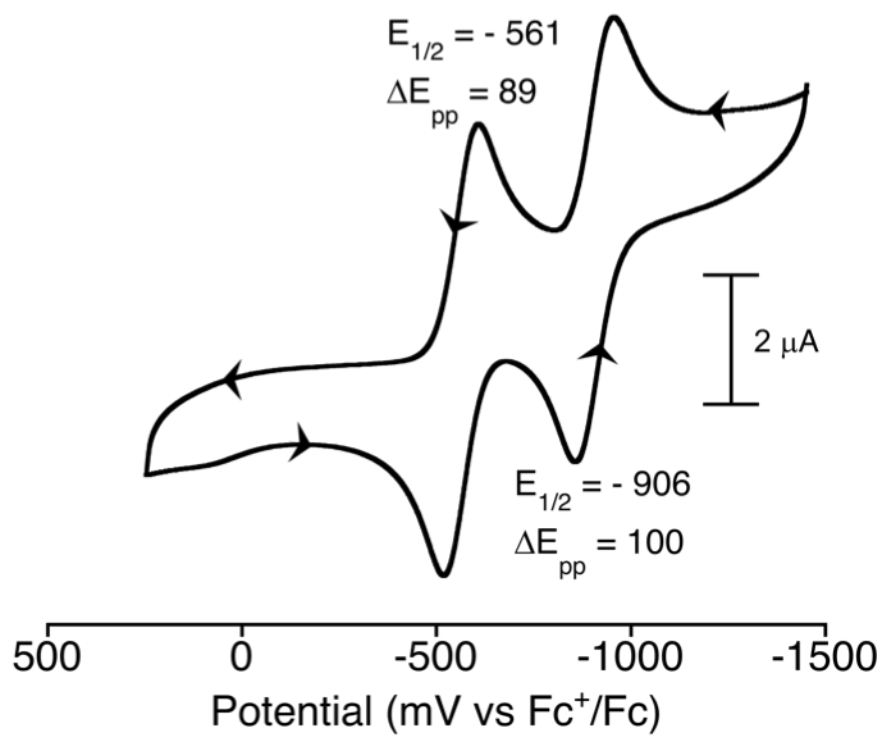
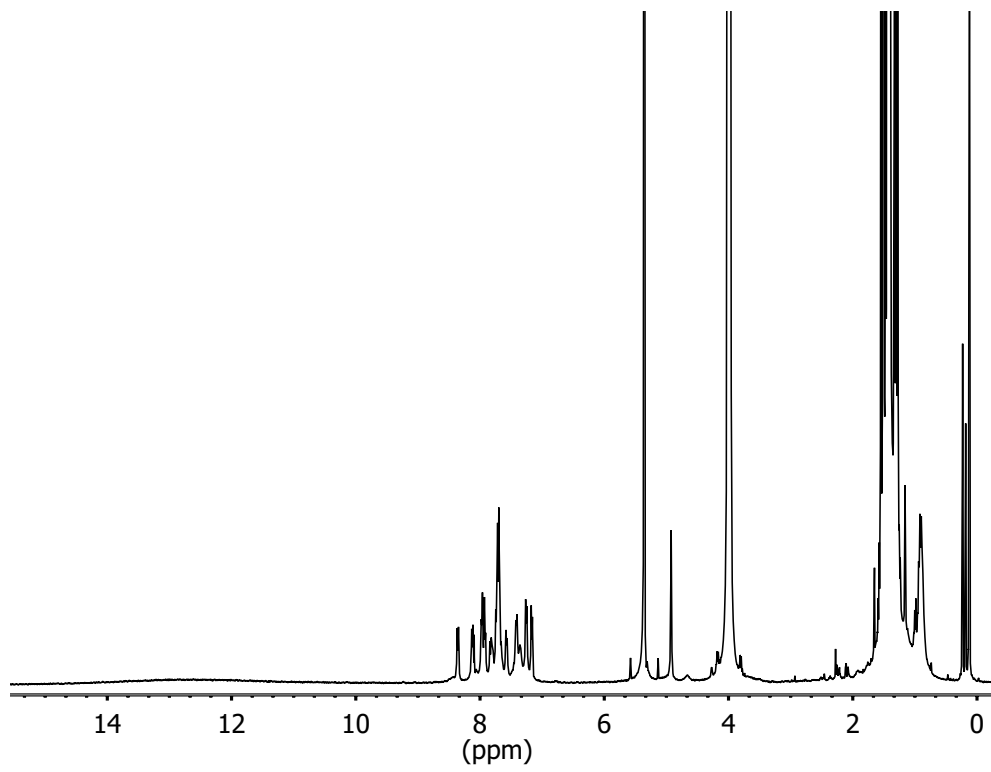
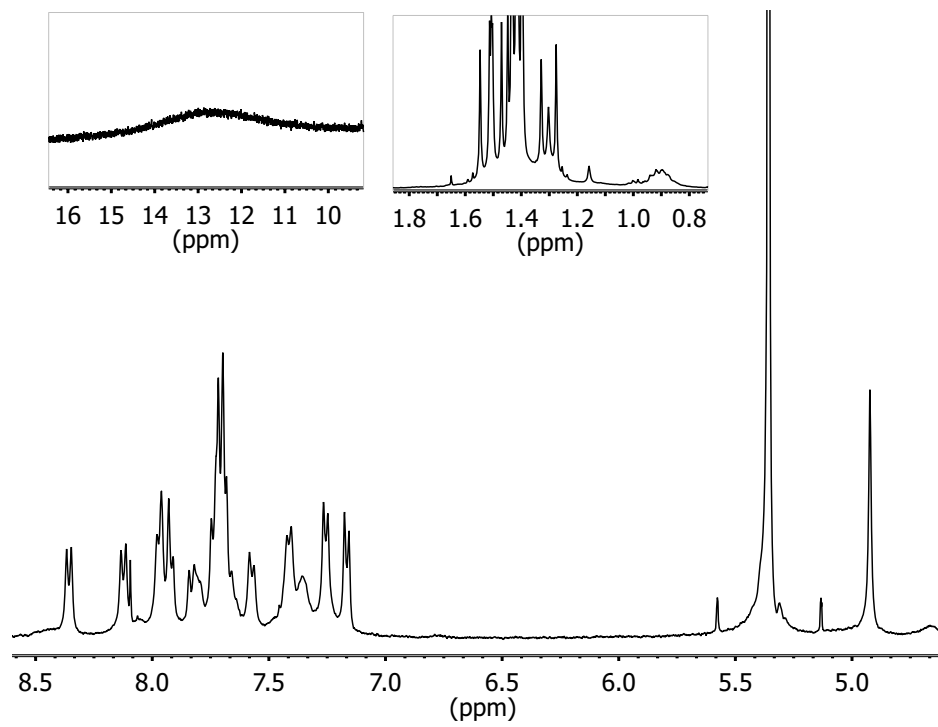


Figure S4. Cyclic voltammogram for $[\text{Re}^{\text{V}}(\text{O})(N\text{-MeTBP}_8\text{Cz})]^+[\text{OTf}]^-$ (**1**) (0.8 mM) in CH_2Cl_2 with 0.1 M $\text{Bu}_4\text{N}^+\text{PF}_6^-$ electrolyte at 50 mV s^{-1} scan rate.

a)



b)



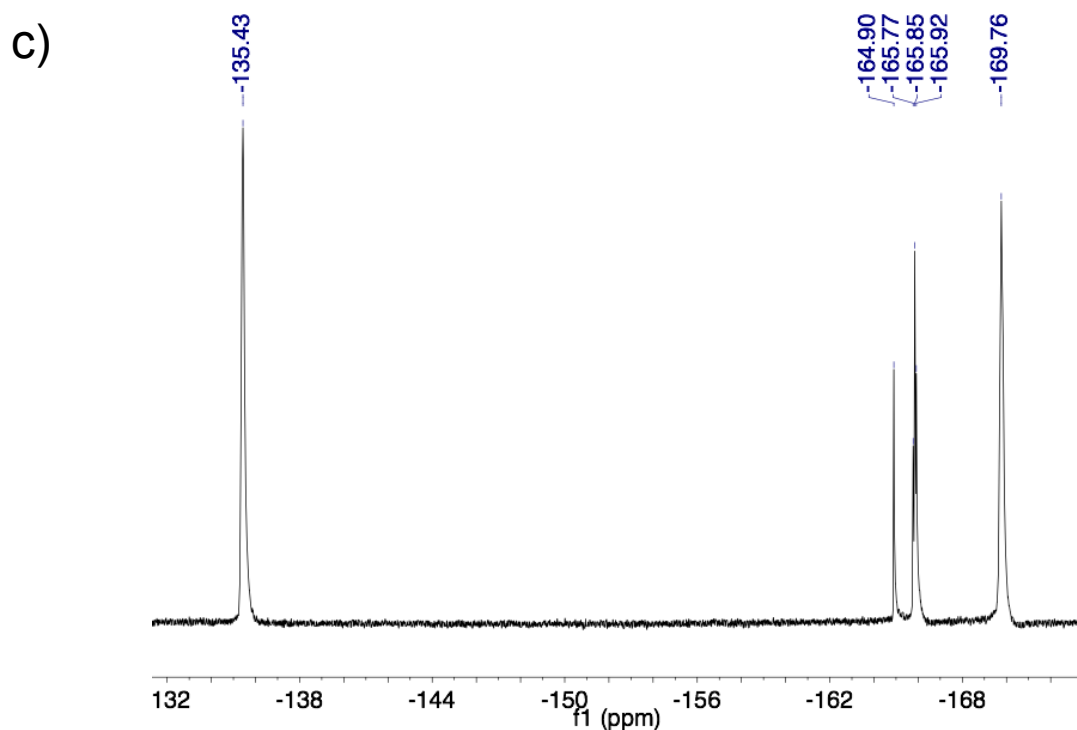


Figure S5. a) ^1H NMR spectrum of in situ generated $[\text{Re}^{\text{V}}(\text{O})(N\text{-MeTBP}_8\text{Cz})(\text{H})]^{2+}[\text{BArF}]_2^-$ (**2**) from $[\text{Re}^{\text{V}}(\text{O})(N\text{-MeTBP}_8\text{Cz})]^+[\text{BArF}]^-$ and HBarF in CD_2Cl_2 . Note: Large peaks at ~ 4 ppm and ~ 1.4 ppm are associated with the Et_2O proton resonances in $\text{HBarF}\cdot 2\text{Et}_2\text{O}$. b) Expansions of selected NMR regions c) ^{19}F NMR spectrum of **2** in CD_2Cl_2 . Chemical shifts were calibrated versus the standard C_6F_6 at -164.9 ppm and the remaining resonances (-135 , -165 , and -169 ppm) represent the three distinctive F-atoms of $[\text{B}(\text{C}_6\text{F}_5)_4]^-$.

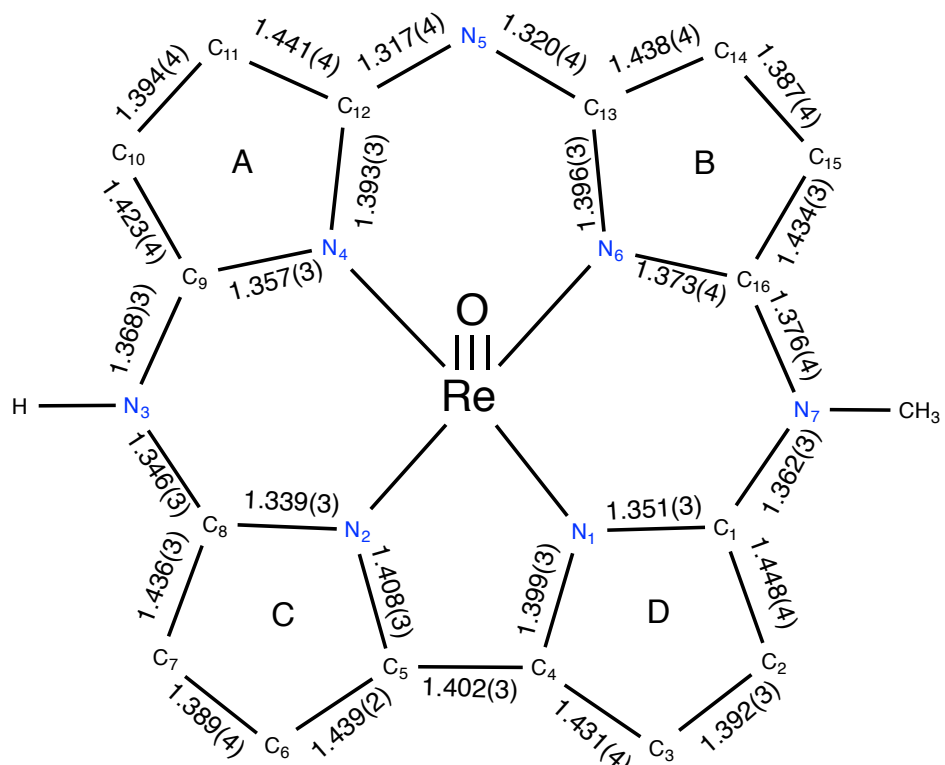


Figure S6. Bond lengths for the macrocyclic core of $[\text{Re}^{\text{V}}(\text{O})(N\text{-MeTBP}_8\text{Cz})(\text{H})]^{2+}[\text{BArF}]_2^-$ (**2**) determined by X-ray crystallography.

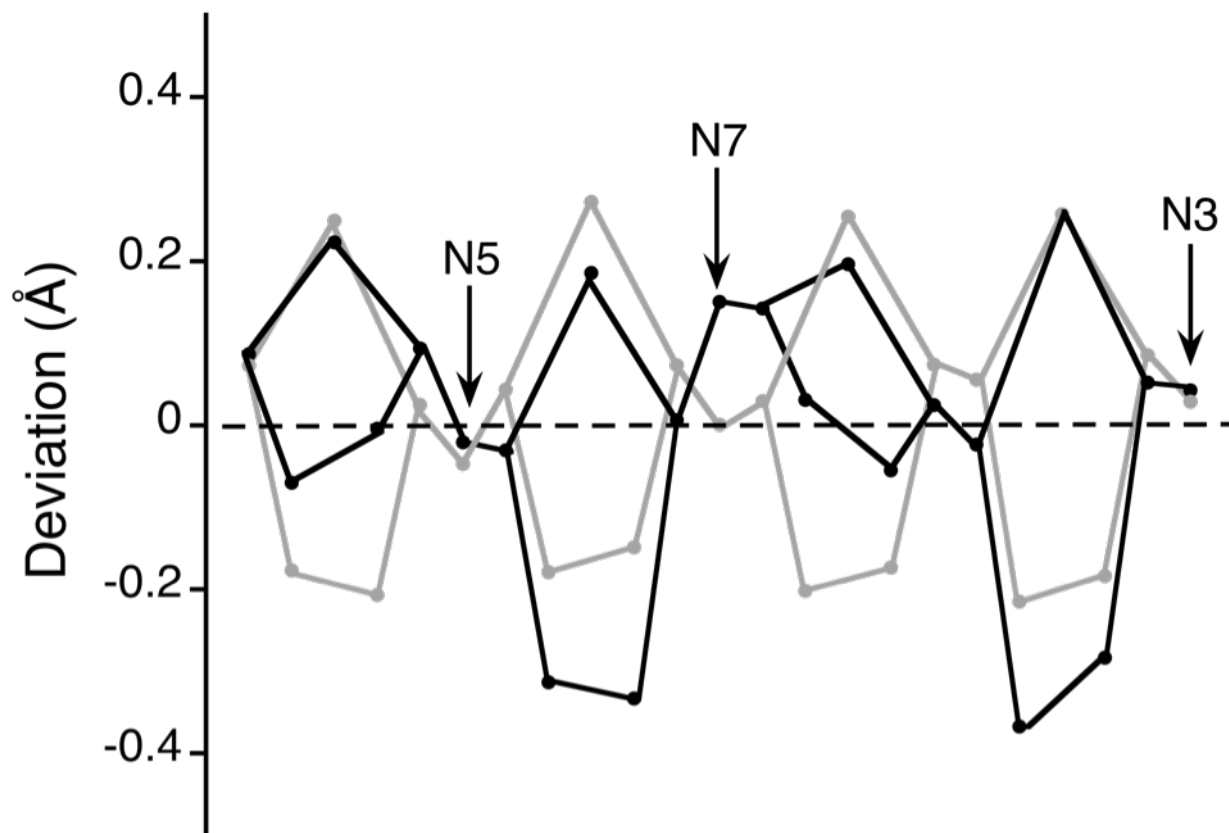


Figure S7. Linear display of deviations (Å) of the macrocycle atoms from the least-squares plane of the 23 atom core for $[\text{Re}^{\text{V}}(\text{O})(N\text{-MeTBP}_8\text{Cz})(\text{H})]^{2+}[\text{BARF}]_2^-$ (**2**) (black) and $\text{Re}^{\text{V}}(\text{O})(\text{TBP}_8\text{Cz})$ (grey).

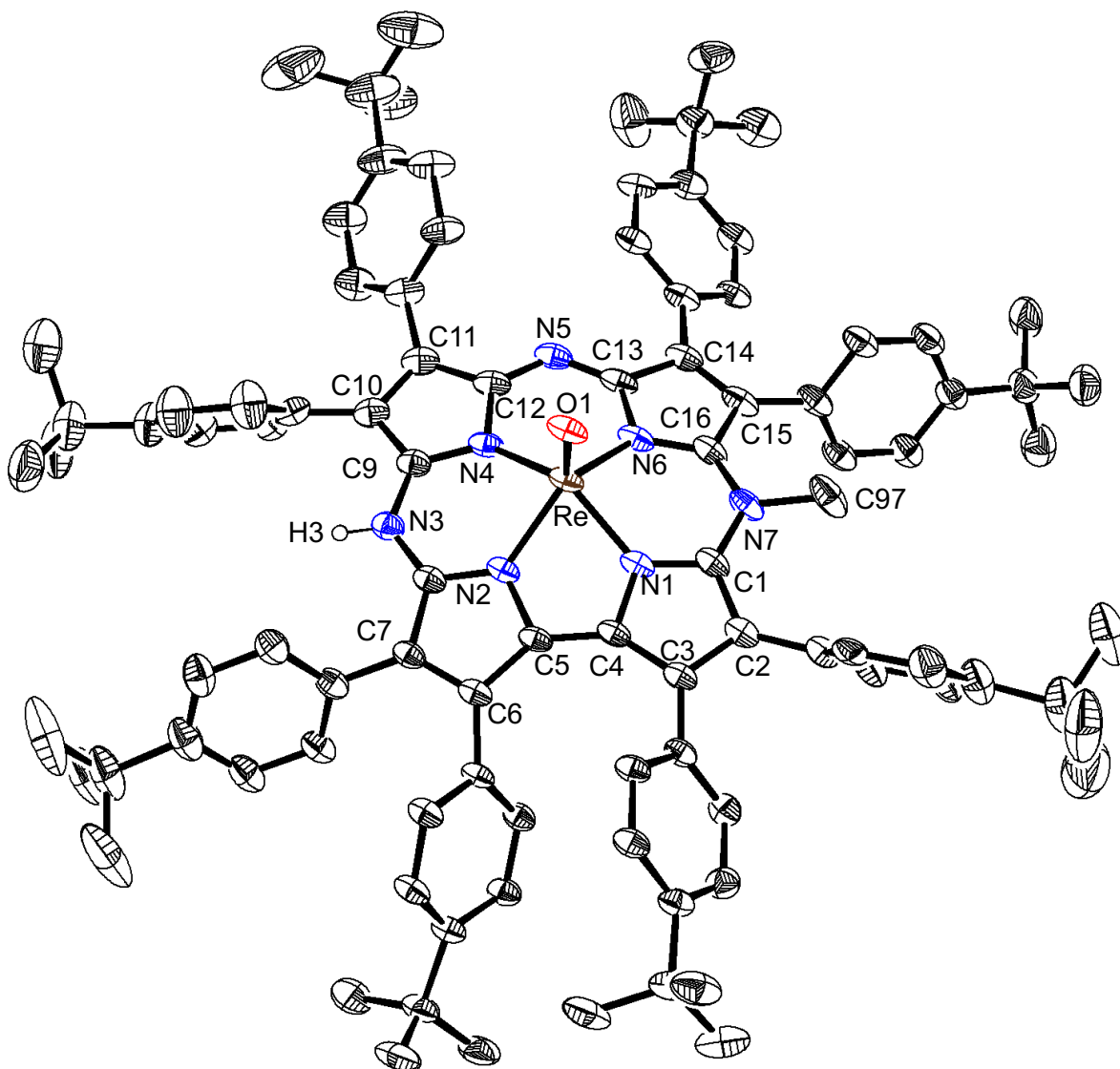


Figure S8. Displacement ellipsoid plot (40% probability level) at 110(2) K of the cation of $[\text{Re}^{\text{V}}(\text{O})(N\text{-MeTBP}_8\text{Cz})(\text{H})]^{2+}[\text{BArF}]_2^-$ (**2**) with selected atoms labeled. H atoms, except for H3, and disorder were omitted for clarity.

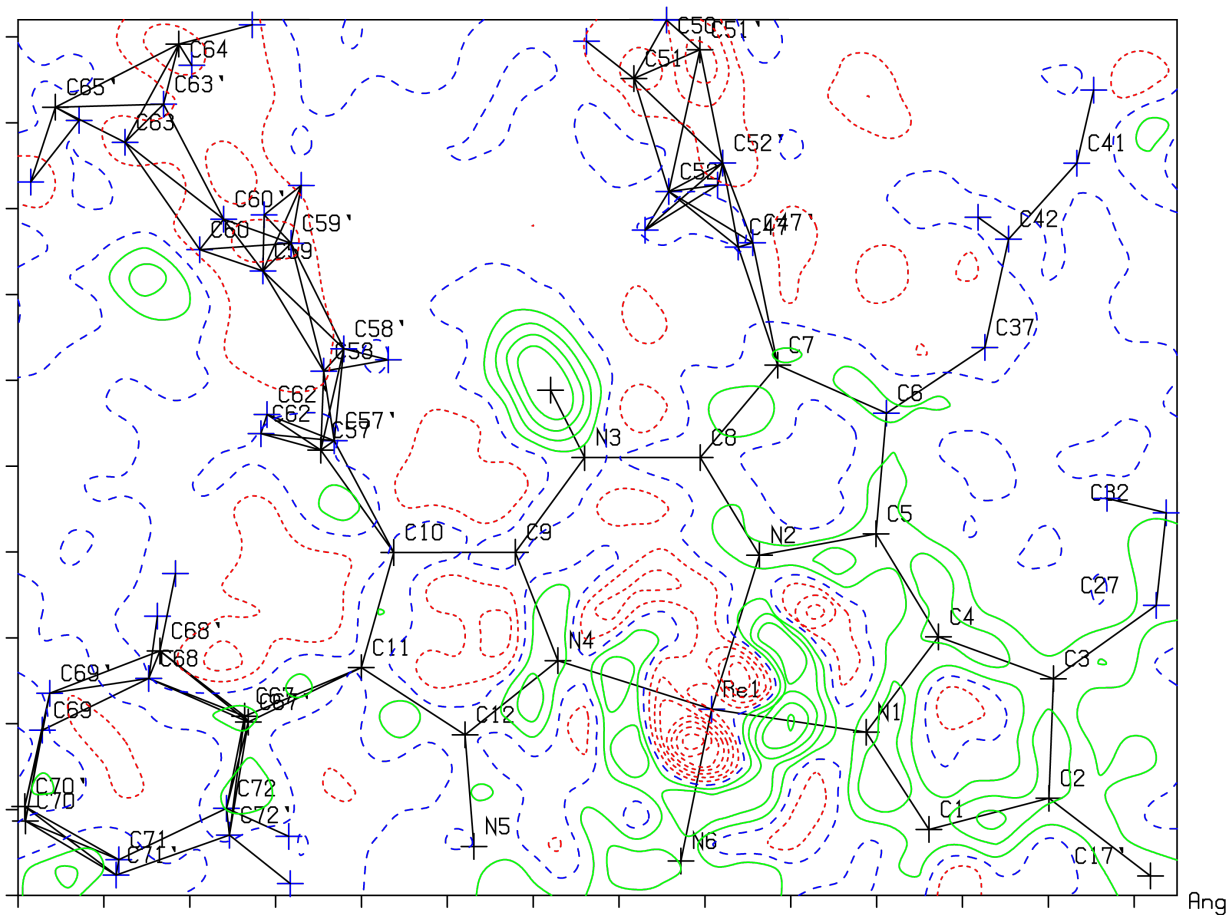


Figure S9. Contoured difference Fourier map drawn in the plane C8–N3–C9 showing the H atom attached to N3 in $[\text{Re}^{\text{V}}(\text{O})(N\text{-MeTBP}_8\text{Cz})(\text{H})]^{2+}[\text{BArF}]_2$ (**2**).

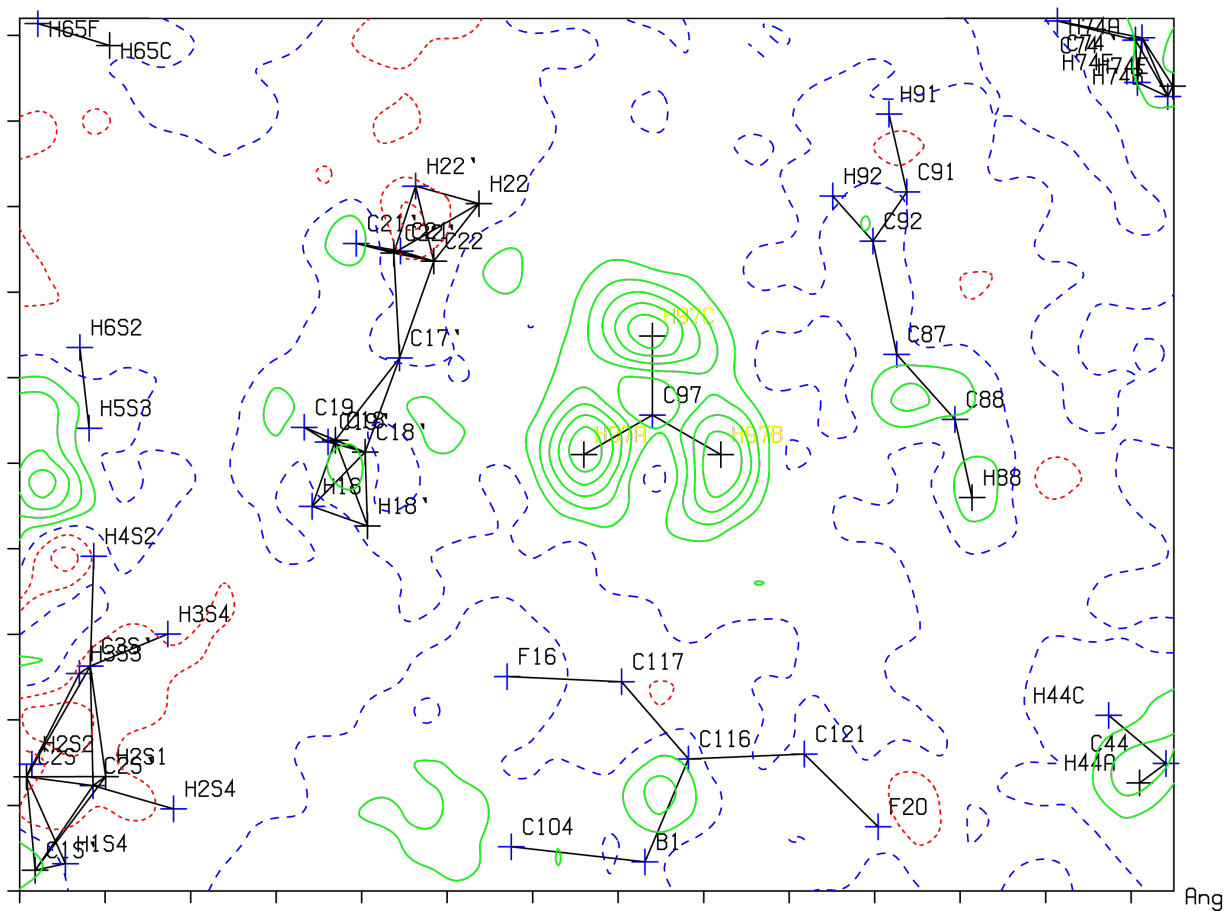


Figure S10. Contoured difference Fourier map showing the three H atoms attached to C97 in $[\text{Re}^{\text{V}}(\text{O})(N\text{-MeTBP}_8\text{Cz})(\text{H})]^{2+}[\text{BArF}]_2$ (**2**).

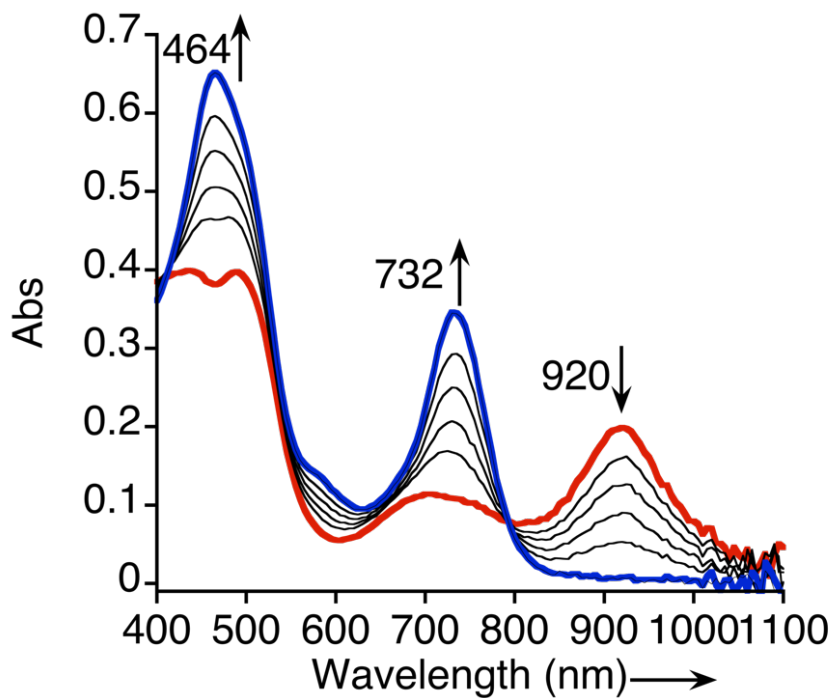


Figure S11. UV-vis spectral titration of $[\text{Re}^{\text{V}}(\text{O})(\text{N-MeTBP}_8\text{Cz})]^+$ (**3**) + $[(\text{C}_5\text{H}_5)_2\text{Fe}][\text{PF}_6]$ (0 – 1 equiv) in CH_2Cl_2 .

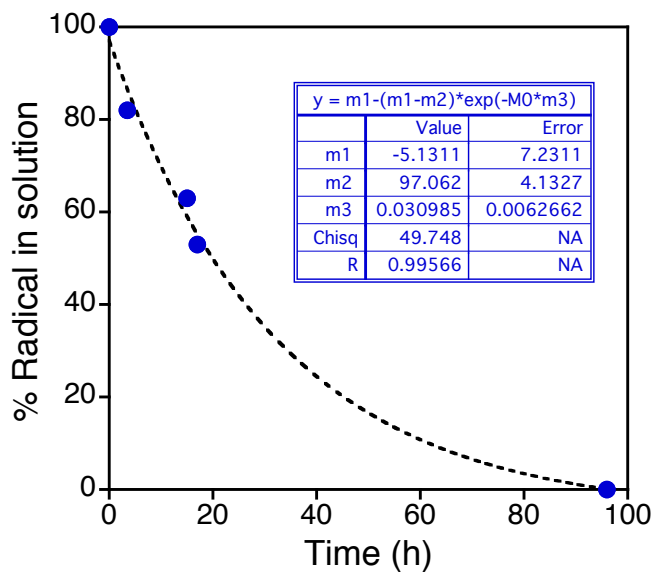


Figure S12. Stability of solid radical **3** in air. Concentration of **3** was obtained from UV-vis measurements, after dissolving the solid in dry CH_2Cl_2 .

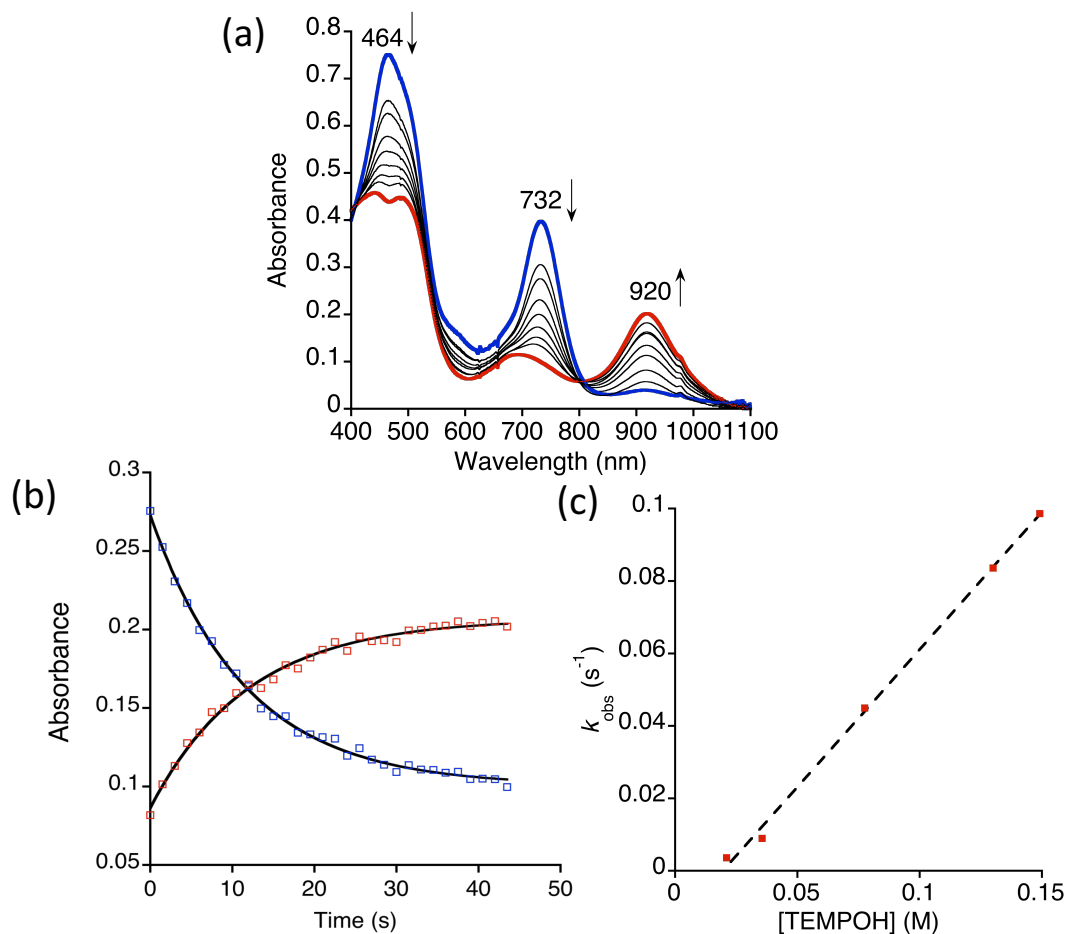


Figure S13. a) Time-resolved UV-vis spectral changes observed for the reaction of $[\text{Re}^{\text{V}}(\text{O})(\text{N-MeTBP}_8\text{Cz})]^+[\text{OTf}]^-$ (1) (16 μM) with TEMPOH (0.13 M) in CH_2Cl_2 at 25 $^\circ\text{C}$. b) Plot of the change in absorbance vs time for the growth of $[\text{Re}^{\text{V}}(\text{O})(\text{N-MeTBP}_8\text{Cz})]^\bullet$ (red squares) and decay of $[\text{Re}^{\text{V}}(\text{O})(\text{N-MeTBP}_8\text{Cz})]^+[\text{OTf}]^-$ (1) (blue circles) with the best fit lines (black). c) Plot of pseudo-first-order rate constants (k_{obs}) vs [TEMPOH] ($R^2 = 0.99$). Slope: $k_2 = 0.76(2) \text{ M}^{-1} \text{ s}^{-1}$.

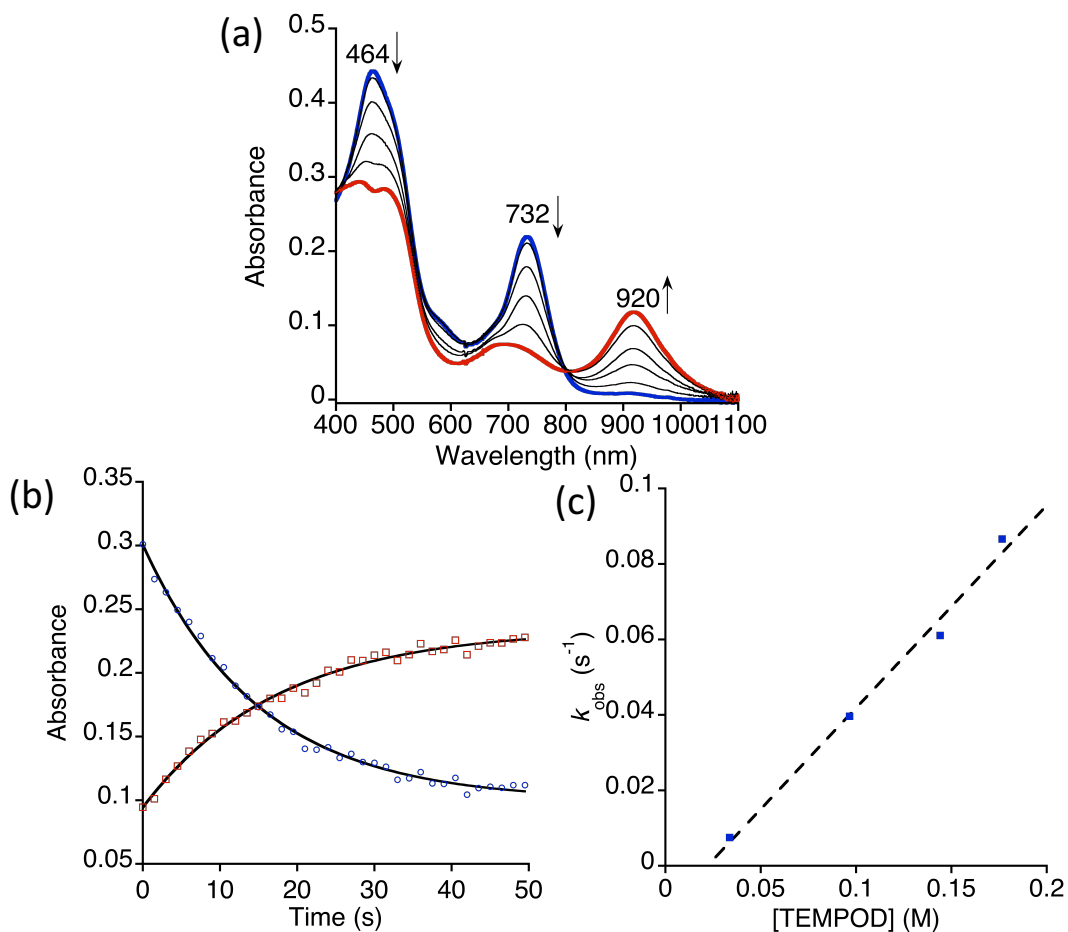


Figure S14. a) Time-resolved UV-vis spectral changes observed for the reaction of $[\text{Re}^{\text{V}}(\text{O})(\text{N-MeTBP}_8\text{Cz})]^+[\text{OTf}]^-$ (1) (13 μM) with TEMPO (0.14 M) in CH_2Cl_2 at 25 $^\circ\text{C}$. b) Plot of the change in absorbance vs time for the growth of $[\text{Re}^{\text{V}}(\text{O})(\text{N-MeTBP}_8\text{Cz})]^\bullet$ (red squares) and decay of $[\text{Re}^{\text{V}}(\text{O})(\text{N-MeTBP}_8\text{Cz})]^+[\text{OTf}]^-$ (1) (blue circles) with the best fit lines (black). c) Plot of pseudo-first-order rate constants (k_{obs}) vs [TEMPO] ($R^2 = 0.99$). Slope: $k_2 = 0.54(4) \text{ M}^{-1} \text{ s}^{-1}$.

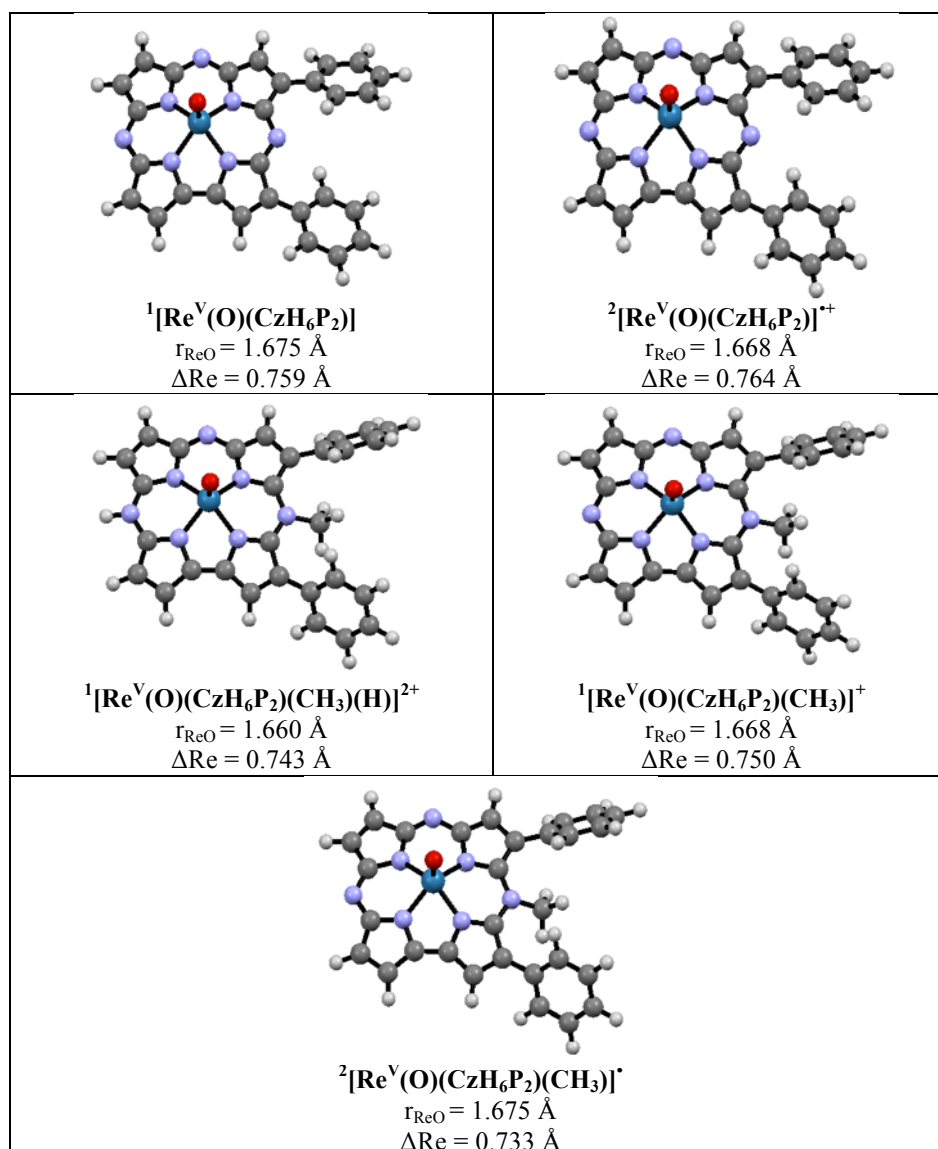


Figure S15. Optimized geometries for singlet ($S = 0$) $^1[\text{Re}^{\text{V}}(\text{O})(\text{CzH}_6\text{P}_2)]$, $^1[\text{Re}^{\text{V}}(\text{O})(\text{CzH}_6\text{P}_2)(\text{CH}_3)(\text{H})]^{2+}$, and $^1[\text{Re}^{\text{V}}(\text{O})(\text{CzH}_6\text{P}_2)(\text{CH}_3)]^+$; and doublet ($S = 1/2$) $^2[\text{Re}^{\text{V}}(\text{O})(\text{CzH}_6\text{P}_2)]^+$ and $^2[\text{Re}^{\text{V}}(\text{O})(\text{CzH}_6\text{P}_2)(\text{CH}_3)]^{\cdot}$. Re–O bond distance (r_{ReO}) and Re–Cz out-of-plane displacement (plane defined by the four internal nitrogens) (ΔRe) are shown in angstroms.

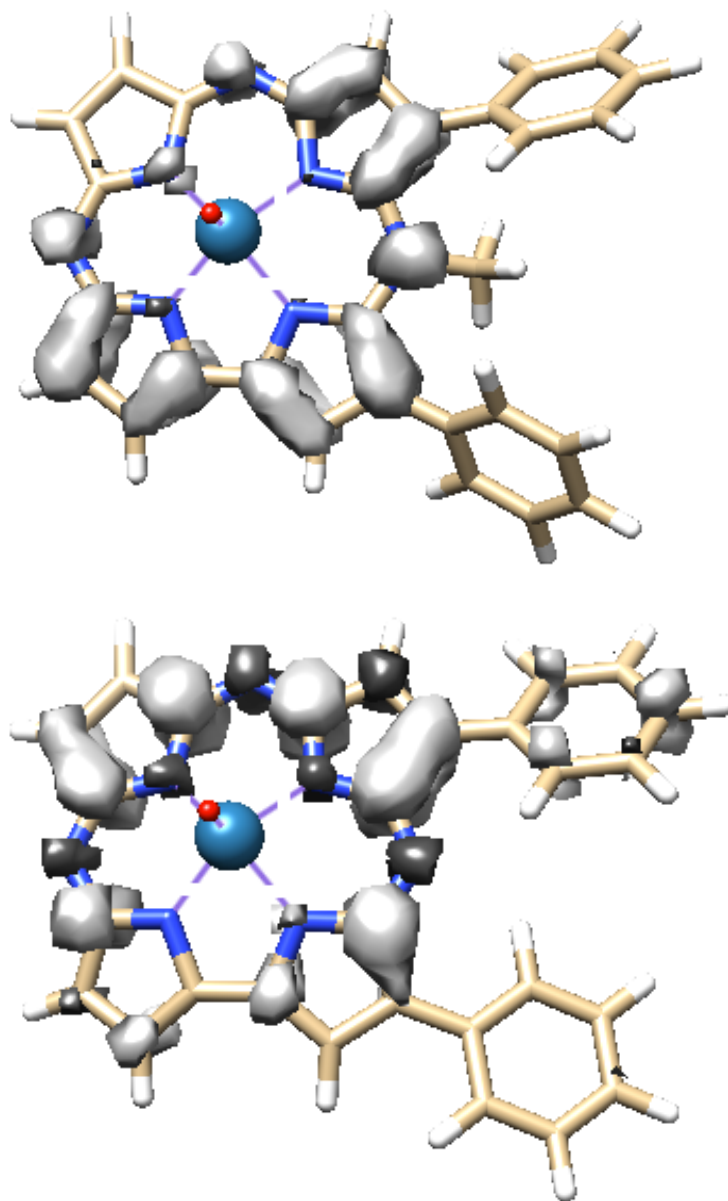


Figure S16. Spin density plot for $^2[\text{Re}^{\text{V}}(\text{O})(\text{CzH}_6\text{P}_2)(\text{CH}_3)]^\bullet$ (top) and $^2[\text{Re}^{\text{V}}(\text{O})(\text{CzH}_6\text{P}_2)]^{2+}$ (bottom) at the PBE0/SDD/6-31G** level of theory. Positive (grey) and negative (black) spin densities are shown at the isodensity level of 0.002 electron/bohr.

Cartesian Coordinates of Optimized Geometries reported:

¹[Re^V(O)(C₂H₆P₂)]

Re	0.00818794032515	0.14933948138561	-0.04790964681023
O	1.52858575437192	0.68049749672875	0.41257645127756
N	-1.27738488166067	0.08869802972508	1.45737135237072
C	-1.52499725166527	-0.88732182443656	2.38136362726643
C	-2.45404279805976	-0.34161280847188	3.34553654925142
C	-2.79636610410977	0.93349059629091	2.89056306608684
C	-2.08611439097749	1.18414564562655	1.69794477279927
C	-2.07358115415102	2.08148004659300	0.60959669950914
C	-2.75809670161129	3.22486805790541	0.12601251565268
C	-2.37319308995706	3.41221989595501	-1.19126440725460
C	-1.46366829332784	2.36865932603690	-1.54125113269089
N	-1.25777392826445	1.62689159067230	-0.40960083820195
N	-0.98933074760538	2.05530446984394	-2.74654846762225
C	-0.39305656979028	0.89321244679940	-2.95497816930338
C	-0.02827355431124	0.38582428416594	-4.24925590754690
C	0.39725502307911	-0.90265906521274	-4.09707599629458
C	0.31168612989959	-1.23143061616071	-2.70241732054572
N	-0.12010245245282	-0.10538834855346	-2.02223448996187
N	0.54000724883625	-2.42815642707173	-2.18825197098915
C	0.28043127263327	-2.71859088802873	-0.91900343926388
C	0.34329811051377	-4.02014402715751	-0.34663668349761
C	-0.08786873528290	-3.95052837604014	0.96111673020228
C	-0.43805701021736	-2.56476187794952	1.20729060256836
N	-0.15056839419412	-1.83677820950067	0.05837052756298
N	-1.05618695675244	-2.12672977183169	2.29322623865391
C	-0.23436453609087	-5.05997712961293	1.90350525311503
C	-0.12552416268421	-4.86865929275918	3.28962709720429
C	-0.24332884248781	-5.94536802864032	4.16116670713341
C	-0.46969563027753	-7.22899300604114	3.67051790870708
C	-0.58157656903525	-7.43081882828886	2.29638284730425
C	-0.46645062392481	-6.35785487898264	1.42256057205181
H	-0.58147067968841	-6.51857760855959	0.35413406220215
H	-0.76788066475884	-8.42665363830893	1.90462721892228
H	-0.56039874731100	-8.06805318947221	4.35431969022270
H	-0.14955967826140	-5.77950602568436	5.23085126749201
H	0.05360229894931	-3.87221570383563	3.67650017072995
H	0.68019978035992	-4.89334763274999	-0.88741070624073
H	0.71432920322494	-1.60166902791144	-4.85839227226291
H	-0.13988645255862	0.95356344998140	-5.16271818508009
H	-2.72389987021584	4.17278312823310	-1.87510866924258
H	-3.47666809785601	3.81434592525784	0.67920720860829
H	-3.53228250053194	1.59058899401795	3.33416187473132
C	-2.96762580230485	-0.99682659549805	4.54774307002383
C	-3.00433200113105	-2.39515044672352	4.66991941243495
C	-3.51395937245491	-2.98752846881396	5.81941066198837
C	-3.99630534267331	-2.20446617443350	6.86521222144983
C	-3.95966613863239	-0.81561623895921	6.75767294028094

C	-3.44881154133012	-0.21864999015659	5.61288970635664
H	-3.39522126784415	0.86493822429164	5.55158716569948
H	-4.32166523846267	-0.19537831977669	7.57268234495630
H	-4.39434917018266	-2.67203470579832	7.76130942412074
H	-3.53730808391975	-4.07129837866660	5.89420340198243
H	-2.62913653318367	-3.00861331942170	3.85865968188964

$^2[\text{Re}^{\text{V}}(\text{O})(\text{C}_2\text{H}_6\text{P}_2)]^{++}$

Re	0.05582048077707	0.14735595613116	-0.03849532040224
O	1.58917715966788	0.64423231981343	0.38922743295544
N	-1.20560965002020	0.11042949615581	1.49314375285815
C	-1.49499205543218	-0.86467178843434	2.38120767589621
C	-2.44722785769607	-0.31550270649689	3.35527305707848
C	-2.75842030741891	0.96361797024429	2.91436205094144
C	-2.02409566627487	1.21966556305329	1.73122064566324
C	-2.00918586684192	2.10461855534868	0.65504009644148
C	-2.72959579726861	3.23234398605549	0.15941209141123
C	-2.37557235990163	3.39820606155237	-1.16049780795703
C	-1.44330013698708	2.36010231626647	-1.50367676364889
N	-1.18824248996364	1.65145876557690	-0.37568402186429
N	-0.98617512203961	2.04399675144083	-2.72501306020439
C	-0.40787391958303	0.88573740838376	-2.93758891938256
C	-0.06279259751068	0.36963931341084	-4.25314270930964
C	0.34104962415356	-0.91559500335908	-4.10808419454840
C	0.26646059252102	-1.24472056136962	-2.69796558657551
N	-0.12765587518716	-0.11263032518722	-2.00722658751025
N	0.47584850494324	-2.44634957299992	-2.19811544305953
C	0.23237860797994	-2.73743586640064	-0.92350264415167
C	0.27206993098574	-4.04508223227493	-0.36683422842084
C	-0.11444422249521	-3.97628865120924	0.95242748683842
C	-0.43781722868396	-2.55713960555689	1.20984435452577
N	-0.14363868936090	-1.83616118901404	0.06779729743996
N	-1.04214076142664	-2.11771107653077	2.29501127381328
C	-0.24262259141408	-5.06590940357155	1.89961838858036
C	-0.16077780411649	-4.85152476357990	3.28941064015977
C	-0.23773080531063	-5.92320859993835	4.16705221130673
C	-0.40731733848212	-7.21916780964448	3.68129461396899
C	-0.49707160884059	-7.44447234878174	2.30627109076525
C	-0.41128062907589	-6.38127825717532	1.42356540795498
H	-0.50416885370812	-6.56005210304950	0.35644708783262
H	-0.63856433660930	-8.45164495061854	1.92739413475363
H	-0.46952778326543	-8.05468785510525	4.37195118232204
H	-0.15571283409825	-5.74916367933715	5.23563624842416
H	-0.01955456596068	-3.84758105008963	3.67136943021474
H	0.57608243323614	-4.91718724542019	-0.92749570423094
H	0.63578578795474	-1.62375965528625	-4.87006595794586
H	-0.17602863368623	0.94511529753345	-5.16180854155922
H	-2.74780078845510	4.13805562272753	-1.85559856158480
H	-3.44752456374936	3.81905009821508	0.71632415684143
H	-3.48965396631896	1.62883342266541	3.35249196077192

C	-2.97145230869588	-0.98244526886479	4.53561380028535
C	-3.01563148325904	-2.38484623566847	4.63859749858128
C	-3.55518496663526	-2.98515106293629	5.76792183854816
C	-4.04868913043622	-2.20637559386926	6.81279712952382
C	-4.00006188415055	-0.81432760651855	6.72704635833684
C	-3.46830787085444	-0.20764652180115	5.60052034103141
H	-3.40575185720016	0.87588211128011	5.55551147014327
H	-4.37040042828677	-0.20457945611170	7.54513829189460
H	-4.46629021117123	-2.68088428456285	7.69572497969076
H	-3.59500167299593	-4.06845593955740	5.83133990729478
H	-2.63623140135032	-2.99521052553299	3.82755340726605

${}^1[\text{Re}^{\text{V}}(\text{O})(\text{C}_2\text{H}_6\text{P}_2)(\text{CH}_3)]^+$

Re	0.05819682785620	0.03729005126461	-0.23259303614260
O	1.61743451009652	0.37896788998590	0.25045704160878
N	-1.24306292657343	0.03726143655734	1.27206681929780
C	-1.60065832632186	-0.90105512873700	2.18233112428428
C	-2.43860798307039	-0.26774439097097	3.17732531577186
C	-2.63869401911820	1.03594430949118	2.73731084919309
C	-1.91825884698397	1.22186455839315	1.54215434729060
C	-1.79384370239085	2.15264925965753	0.50153151350703
C	-2.34476217871936	3.39764822006985	0.07846138650236
C	-1.93232972721524	3.60581954416077	-1.21887469411426
C	-1.13949962101422	2.47651159481905	-1.62442991743460
N	-1.02454002949589	1.66030436067623	-0.53299569601397
N	-0.70255195027566	2.17722211701922	-2.83833099168019
C	-0.22785541706810	0.96741338933658	-3.10386464992740
C	0.07824082868017	0.48792690509051	-4.42397337626810
C	0.37027966769818	-0.84267097640528	-4.33307108253739
C	0.25663561132183	-1.21854702959659	-2.95259171196247
N	-0.05967512844331	-0.08768622070557	-2.21739838131117
N	0.37863957720356	-2.44261803155625	-2.48029610580692
C	0.10360485520455	-2.77714675731456	-1.22863603401781
C	0.16165496706032	-4.09105915957819	-0.70461883678414
C	-0.23686820001849	-4.06851736799979	0.61659293438063
C	-0.60451691385380	-2.69977441988485	0.89376624071290
N	-0.31639365230149	-1.92623714774884	-0.20885853313713
N	-1.26508094595157	-2.21314133472837	1.99529269919876
C	-1.82061010321633	-3.19096653707223	2.95036763794060
H	-1.12541076298055	-3.37360763442008	3.76989988169881
H	-2.75232883158924	-2.79679536215636	3.34470164209512
H	-2.01938306879759	-4.12188489693690	2.42897721911077
C	-0.17945008565982	-5.25022106802863	1.49783429337054
C	0.61133354365189	-5.24258204355694	2.65493807708812
C	0.71764771497183	-6.38621250745443	3.43774830680643
C	0.03892065277799	-7.54864135119723	3.07541758309558
C	-0.73977337009454	-7.56702769339408	1.92159594000920
C	-0.84614385416301	-6.42580853888261	1.13212005336631
H	-1.45440287228897	-6.43840765788917	0.23188267900356
H	-1.26402563202877	-8.47235578631483	1.63196581648667

H	0.12490808642370	-8.44094151284556	3.68791490113139
H	1.34202000962687	-6.37526082918344	4.32603151938305
H	1.16758207554844	-4.34741595575564	2.92247205063444
H	0.50970647428668	-4.95414171447461	-1.25505526537093
H	0.61554044369976	-1.53437427392913	-5.12702446381165
H	0.02517231185831	1.10656036096853	-5.30927132409860
H	-2.18365444625446	4.43655580926574	-1.86400041153545
H	-2.99064365404457	4.03732943529937	0.66429322924262
H	-3.23594740135392	1.77591215823509	3.25254562885379
C	-2.98444203069907	-0.77264948612395	4.45193588794164
C	-2.13183073281700	-1.19016011778897	5.48332031307430
C	-2.65709766970784	-1.59320515719415	6.70536829384283
C	-4.03563424196954	-1.58566022575087	6.91200485762937
C	-4.88836443222045	-1.16496193164391	5.89512450552772
C	-4.36747038620443	-0.75449243150719	4.67154031543304
H	-5.03217733786591	-0.43003914410734	3.87565735959386
H	-5.96259829385722	-1.15378527109714	6.05344377185909
H	-4.44312283048226	-1.90198034330724	7.86713841786608
H	-1.98882168087646	-1.90298138370360	7.50295383336232
H	-1.05508263997900	-1.17070808934819	5.33430875475945

$^1[\text{Re}^{\text{V}}(\text{O})(\text{CzH}_6\text{P}_2)(\text{CH}_3)(\text{H})]^{2+}$

Re	-0.05284767723941	-0.00510976932194	0.00968060632378
O	1.47863038363323	0.36271338843346	0.53505469496837
N	-1.38321253104360	-0.03353290863358	1.48070973083156
C	-1.72263326127197	-0.97266535521512	2.39715460743587
C	-2.57471185240164	-0.339583925556628	3.40316441728670
C	-2.81848404925367	0.94555301695350	2.93740104295231
C	-2.09885951248395	1.13449654205771	1.74074601251468
C	-1.97554194081760	2.07558609943723	0.71278241649466
C	-2.54109831664093	3.30769496758237	0.28684795231144
C	-2.09955745649987	3.54681500726514	-1.00233666391517
C	-1.27612624616293	2.44342841846504	-1.36413599991204
N	-1.16401462017436	1.60876780960010	-0.31389845905420
N	-0.73782996009210	2.09732076254941	-2.56167099643027
C	-0.23533432833682	0.88039141734760	-2.88786732015500
C	0.12715455716805	0.43595797322287	-4.19322188931676
C	0.43222804449583	-0.89524713354113	-4.08146431752848
C	0.26130512143523	-1.27284743562070	-2.70872503160402
N	-0.10984892649458	-0.13637614547153	-1.98916580348246
N	0.37151229503907	-2.48519910628491	-2.22057993484133
C	0.06387040132970	-2.82654367116477	-0.97815582203414
C	0.10485674355779	-4.14276570373382	-0.46485565004640
C	-0.31375331083708	-4.12674340258739	0.85259441423835
C	-0.68818770089247	-2.75476908930316	1.12430204703872
N	-0.37258292074376	-1.97280626544207	0.03573818594989
N	-1.38193927852726	-2.27687505168080	2.21248542255046
C	-1.98411279527496	-3.27680724751630	3.12773429756100
H	-1.29444965319921	-3.53203841122386	3.93017104078556
H	-2.89638025859683	-2.85765657808260	3.54073697630231

H	-2.22187527101673	-4.16959696898652	2.55607942632363
C	-0.27315231513553	-5.30406735041580	1.73116842382127
C	0.45600609813556	-5.27521009150940	2.93019451740845
C	0.56495908207593	-6.42240395419275	3.70540613895677
C	-0.05612757882435	-7.60368413717774	3.29835982732537
C	-0.77510862395923	-7.64074305953894	2.10593087382571
C	-0.87735588312094	-6.49966782803328	1.31737200883839
H	-1.43770199582081	-6.52864073856313	0.38698080329450
H	-1.25263449089449	-8.56107135962883	1.78569423810587
H	0.03063692898004	-8.49835914714703	3.90699942390052
H	1.14820571626660	-6.40235782206861	4.62061600575067
H	0.97599855844486	-4.36791645005421	3.22922512293973
H	0.46083518765585	-5.00385583897917	-1.01431457099425
H	0.72539700163940	-1.57734016281948	-4.86832402315916
H	0.11770370461034	1.03914722105209	-5.09210362932920
H	-0.80590025538720	2.77319335747503	-3.31550278253736
H	-2.35915417337634	4.38755635730492	-1.63221762673639
H	-3.21666572582434	3.93301093915000	0.85523176352682
H	-3.42204819742545	1.68404570119496	3.44779877700198
C	-3.06804820247580	-0.83346940508729	4.69138324669238
C	-2.18376967094429	-1.36624991593667	5.64515375928091
C	-2.65052260042557	-1.72553563493116	6.90174075836676
C	-4.00157784569949	-1.57231882933793	7.21687968376535
C	-4.88470146896142	-1.04403739680030	6.27699097859333
C	-4.42177096657812	-0.66342169166391	5.02329478410466
H	-5.11197437927999	-0.25818459118020	4.28849393425682
H	-5.93521446582205	-0.92562295494707	6.52229882516514
H	-4.36385363702519	-1.86006196103071	8.19863840180784
H	-1.95968251520229	-2.11330495319819	7.64358638444821
H	-1.12483564428285	-1.45429461547313	5.41586520802987

$^2[\text{Re}^{\text{V}}(\text{O})(\text{C}_2\text{H}_6\text{P}_2)(\text{CH}_3)]^+$

Re	-0.01115156000908	0.01932484573487	-0.24358716152847
O	1.54358296882731	0.36755325471353	0.27299509578907
N	-1.32478488066647	0.01707449853178	1.24778328736326
C	-1.66810009314980	-0.91997302824345	2.17047603611990
C	-2.46362690528249	-0.29406587900001	3.16826880859151
C	-2.66290190758207	1.03784958020399	2.73264932710208
C	-1.97224515620875	1.21499136701374	1.54187038776409
C	-1.83498697405236	2.16071076326502	0.48467991961295
C	-2.35091902042957	3.39873906050020	0.06783893987312
C	-1.92300198193090	3.60588614794308	-1.24692276714173
C	-1.16025692200583	2.48091859643407	-1.64107923317431
N	-1.08020491179449	1.64936838097892	-0.55297149174538
N	-0.68191645105158	2.17537338410831	-2.86065332640666
C	-0.21892681811743	0.97245404521194	-3.10945870055982
C	0.14762509592858	0.49702871299758	-4.42656305597069
C	0.44516313082375	-0.82494703357194	-4.33710118930866
C	0.28125979603391	-1.22650529884143	-2.95868965384767

N	-0.07572771236005	-0.09768483270086	-2.22758762954755
N	0.41454783754591	-2.44335063808084	-2.50604922024205
C	0.11004618264414	-2.79700261383661	-1.24535242008320
C	0.18187660276970	-4.09080782383950	-0.72409521341779
C	-0.25401674242626	-4.06423042593844	0.60647624717742
C	-0.64602002285727	-2.72395784273407	0.86545847318053
N	-0.36005788585520	-1.94993579497985	-0.23820748297903
N	-1.34686856858404	-2.24887918057041	1.96769589457666
C	-2.08002297686934	-3.23403827849447	2.76776520718896
H	-1.52265247363496	-3.55262283330910	3.65021281010283
H	-3.02339322621820	-2.79329223347293	3.08352254869873
H	-2.28781072782862	-4.10505109610164	2.14936155330060
C	-0.17498947023594	-5.22252665311655	1.51175683249098
C	0.45747396204530	-5.12368393086497	2.75949210996342
C	0.58125275721268	-6.23683322992237	3.58345673499826
C	0.08449619091589	-7.47203341304806	3.17261804872309
C	-0.53238782197698	-7.58627032576317	1.92944886671438
C	-0.66040082248906	-6.47250603301110	1.10562053175071
H	-1.15015067871464	-6.56101207817198	0.13990963828250
H	-0.91973698421295	-8.54612069976955	1.60027735638700
H	0.18398153985238	-8.34189259297640	3.81527130553036
H	1.07911849293408	-6.14265233918011	4.54421642596165
H	0.87484593372581	-4.16843084518194	3.06782081243869
H	0.56425502761682	-4.94992252882721	-1.25698429298581
H	0.72882057603408	-1.50768536743034	-5.12620333006502
H	0.12652268551097	1.12545946927755	-5.30646409621194
H	-2.15805789417391	4.44376240466266	-1.88822708883860
H	-2.98704036846417	4.05162046592131	0.64992605889464
H	-3.23307368200680	1.78422409344287	3.26869739942217
C	-2.95641039759215	-0.79326133539222	4.46261264862602
C	-2.09419913268995	-1.40324929053156	5.38583875583901
C	-2.56060972411413	-1.81639033398545	6.62882290818469
C	-3.89457712745315	-1.61801493595739	6.97935798732293
C	-4.75777789464089	-1.00024935483146	6.07781478374630
C	-4.29369449863936	-0.59127620514487	4.83171169645344
H	-4.97198531631003	-0.12271678967266	4.12370452628914
H	-5.79872857430875	-0.83954910474556	6.34326910458154
H	-4.25716737149405	-1.93836049980347	7.95136907648279
H	-1.87633603866151	-2.28181789250004	7.33260134719896
H	-1.04604883332818	-1.52982396739744	5.12843639132998

References:

- (1) J. P. T. Zaragoza, M. A. Siegler, and D. P. Goldberg, *Chem. Commun.* 2016, **52**, 167.
- (2) P. Jutzi, C. Müller, A. Stammler and H.-G. Stammler, *Organometallics* 2000, **19**, 1442.
- (3) S. Marque, H. Fischer, E. Baier and A. Studer, *J. Org. Chem.* 2001, **66**, 1146.
- (4) F. Neese, *Wiley Interdiscip. Rev. Comput. Mol. Sci.* 2012, **2**, 73.
- (5) C. Adamo and V. Barone, *J. Chem. Phys.* 1999, **110**, 6158.
- (6) M. Ernzerhof and G. Scuseria, *J. Chem. Phys.* 1999, **110**, 5029.
- (7) L. E. Roy, P. J. Hay and R. L. Martin, *J. Chem. Theory Comput.* 2008, **4**, 1029.
- (8) P. C. Hariharan and J. A. Pople, *Theor. Chim. Acta* 1973, **28**, 213.
- (9) M. M. Francl, *J. Chem. Phys.* 1982, **77**, 3654.
- (10) D. W. Demoin, Y. Li, S. S. Jurisson and C. A. Deakyne, *Comput. Theor. Chem.* 2012, **997**, 34.
- (11) G. M. Sheldrick, *Acta Crystallogr. Sect. C Struct. Chem.* 2015, **71**, 3.
- (12) A. L. Spek, *Acta Crystallogr. D Biol. Crystallogr.* 2009, **65**, 148.